

Correlation between Bonding Geometry and Band Gap States at Organic–Inorganic Interfaces: Catechol on Rutile TiO₂(110)

Shao-Chun Li,[†] Jian-guo Wang,[‡] Peter Jacobson,[†] X.-Q. Gong,[‡]
Annabella Selloni,^{*‡} and Ulrike Diebold^{*†}

Department of Physics, Tulane University, New Orleans, Louisiana 70118, and Department of Chemistry, Princeton University, Princeton, New Jersey 08544

Received May 21, 2008; E-mail: aselloni@princeton.edu; diebold@tulane.edu

Abstract: Adsorbate-induced band gap states in semiconductors are of particular interest due to the potential of increased light absorption and photoreactivity. A combined theoretical and experimental (STM, photoemission) study of the molecular-scale factors involved in the formation of gap states in TiO₂ is presented. Using the organic catechol on rutile TiO₂(110) as a model system, it is found that the bonding geometry strongly affects the molecular electronic structure. At saturation catechol forms an ordered 4 × 1 overlayer. This structure is attributed to catechol adsorbed on rows of surface Ti atoms with the molecular plane tilted from the surface normal in an alternating fashion. In the computed lowest-energy structure, one of the two terminal OH groups at each catechol dissociates and the O binds to a surface Ti atom in a monodentate configuration, whereas the other OH group forms an H-bond to the next catechol neighbor. Through proton exchange with the surface, this structure can easily transform into one where both OH groups dissociate and the catechol is bound to two surface Ti in a bidentate configuration. Only bidentate catechol introduces states in the band gap of TiO₂.

1. Introduction

Catechol adsorbed on TiO₂ has received considerable attention in recent years both as a model system for the photocatalytic oxidation of organic pollutants^{1,2} and as a model dye sensitizer for TiO₂-based dye sensitized solar cells (DSSC).^{3,4} Catechol adsorbed on TiO₂ nanoparticles⁵ shows a band in the absorption spectrum at ~430 nm (i.e., below the onset of the band-to-band TiO₂ absorption at ~380 nm, and well below the intramolecular excitation at 300 nm) that is attributed to the indirect excitation from the molecular HOMO in the TiO₂ bandgap to the conduction band of the nanoparticle.⁴ This finding has prompted several theoretical studies of the bonding geometry and molecule–semiconductor charge transfer process by various approaches, including semiempirical quantum-chemical, density functional theory (DFT), and time-dependent quantum methods.^{4,6–8} Other simple aromatic molecules such as benzoic acid do not introduce states into the band gap,^{4,8} making them unsuitable for modeling photoexcited charge transfer.

Given the interest in catechol, there has been little to no atomic scale experimental study of its adsorption geometry on TiO₂ surfaces, possibly because bonding properties similar to

those of the carboxylic acids have been assumed.^{9,10} In this work, we use UV photoemission spectroscopy (UPS), scanning tunneling microscopy (STM), and DFT calculations to investigate the adsorption properties of catechol on the prototype rutile TiO₂(110) surface, which is the best microscopically characterized surface of TiO₂.

Our STM measurements show that catechol molecules form an ordered densely packed monolayer on the TiO₂(110) surface, and UPS finds that this overlayer gives rise to electronic states above the TiO₂ valence band edge in the band gap. DFT calculations can explain these findings by assuming that two structures are simultaneously present: one involving only partially dissociated (monodentate) adsorbed molecules, and the other involving alternating monodentate and bidentate (fully dissociated) molecules. The first structure is computed to be most stable, but the mixed monodentate–bidentate structure, which is the next most stable one and 0.18 eV/molecule higher in energy, is essential to explain the UPS data. Our calculations further suggest that the two monolayer structures can easily transform one into the other via proton exchange with the surface. Both finite temperature entropic effects and the reduction of the TiO₂ sample (not accounted for in our calculations) may contribute to the stabilization of the mixed monolayer structure.

[†] Tulane University.

[‡] Princeton University.

- (1) Linsebigler, A. L.; Lu, G.; Yates, J. T., Jr. *Chem. Rev.* **1995**, *95*, 735–758.
- (2) Lana-Villarreal, T.; Monllor-Satoca, D.; Rodes, A.; Gómez, R. *Selected Contributions of the 4th European Meeting on Solar Chemistry and Photocatalysis: Environmental Applications (SPEA 4)* **2007**, *129* (1–2), 86.
- (3) Grätzel, M. *Nature* **2001**, *414*, 338–344.
- (4) Persson, P.; Bergstrom, R.; Lunell, S. *J. Phys. Chem. B* **2000**, *104*, 10348–10351.
- (5) Moser, J.; Punchedewa, S.; Infelta, P. P.; Graetzel, M. *Langmuir* **1991**, *7*, 3012–3018.

- (6) Redfern, P. C.; Zapol, P.; Curtiss, L. A.; Rajh, T.; Thurnauer, M. C. *J. Phys. Chem. B* **2003**, *107*, 11419–11427.
- (7) Rego, L. G. C.; Batista, V. S. *J. Am. Chem. Soc.* **2003**, *125*, 7989–7997.
- (8) Duncan, W. R.; Prezhdo, O. V. *Annu. Rev. Phys. Chem.* **2007**, *58*, 143–184.
- (9) Onishi, H.; Iwasawa, Y. *Chem. Phys. Lett.* **1994**, *226*, 111–114.
- (10) Guo, Q.; Cocks, I.; Williams, E. M. *J. Chem. Phys.* **1997**, *106*, 2924–2931.

2. Experimental and Theoretical Details

Scanning tunneling microscopy (STM) measurements were performed at room temperature and low temperature in an ultrahigh vacuum (UHV) chamber with base pressure of 2×10^{-10} mbar and a variable-temperature STM. Catechol was dosed through a leak valve onto sputtered/annealed TiO₂(110) substrates. Clean and catechol-dosed TiO₂ surfaces were characterized by X-ray photoelectron spectroscopy (XPS) and shown to be free from contaminants. UPS was performed on the 3m TGM beamline at the Center for Advanced Microstructures and Devices (CAMD) in Baton Rouge, LA. All photoemission measurements were taken with 40 eV photons and an analyzer that could be moved about two azimuthal orientations. The TiO₂(110) surface was prepared with standard cleaning procedures involving sputtering and annealing in UHV. Catechol (Alfa Aesar, 99%) was purified through a combination of heating and vacuum sublimation. The as-purchased product is a powder with a light-brown coloration, and after further purification the catechol changed to a light-yellow color. Small amounts of water were evident upon analysis by mass spectrometry. XPS and UPS show no indication of fragmentation of the aromatic ring upon adsorption.

DFT calculations were performed on a 4×1 supercell of a TiO₂(110) slab with four O–Ti–O trilayers, using the PBE exchange-correlation functional,¹¹ within the plane-wave pseudopotential method as implemented in the *Quantum-Espresso* package.¹² Ultrasoft pseudopotentials¹³ included O 2s and 2p and Ti 3s, 3p, 3d, and 4s electrons. Plane-wave basis set cutoffs for the smooth part of the wave functions and the augmented density were 25 and 200 Ry, respectively. A $1 \times 2 \times 1$ mesh of k-points was used to sample the Brillouin zone. Molecules were adsorbed on one side of the slab only, and a vacuum of 15 Å was introduced to separate adjacent replicas. All atomic positions were fully relaxed except the atoms in the bottom trilayer of the TiO₂ slab, which were kept fixed. Geometry optimizations were carried out until the largest component in the ionic forces was less than 0.03 eV/Å. Our theoretical STM images were calculated from the local density of states in the vacuum region¹⁴ at distance of ~ 2.0 Å from the highest molecular apex.

3. Results and Discussion

Parts a–c of Figure 1 show the TiO₂(110) surface with increasing amounts of catechol, dosed at room temperature. The clean TiO₂(110) surface contains a few percent of oxygen vacancies as is typical for this surface. Depending on the vacuum conditions during dosing, these vacancies were partially filled with hydroxyls through dissociation of water from the residual gas before introducing catechol. The experimental results shown here were independent of the degree of surface hydroxylation of O vacancies. At the lowest coverage, STM shows isolated catechol molecules, adsorbed at the undersaturated Ti5c atoms of the TiO₂(110) surface (part a of Figure 1). As the coverage increases, the molecules begin to form pairs and short rows, extended along the $[1\bar{1}0]$ direction (parts b and c of Figure 1). At saturation coverage, STM shows the formation of a well-ordered superstructure with a 4×1 periodicity (Figure 2); this complete monolayer is the focus of the current work. The formation of the (4×1) overlayer was independent of dosing temperature, except for the lowest temperatures (145 K, part d of Figure 1), where catechol forms poorly ordered $[1\bar{1}0]$ -oriented rows, probably due to low mobility. No indication of multilayer formation was observed.

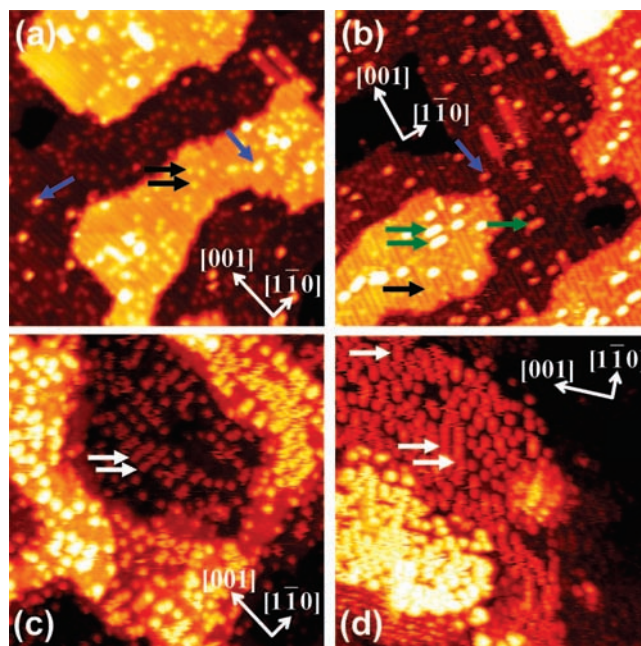


Figure 1. (a–c) STM images (30×30 nm²) of a TiO₂(110) surface with increasing catechol coverage at room temperature and (d) of a saturation coverage of catechol dosed at 145 K. Note that the sample orientation is rotated in (d). Indicated are hydroxyls at bridging oxygen rows (black arrows), isolated catechol molecules (blue arrows), pairs of catechol molecules (green arrows), and $[1\bar{1}0]$ -oriented rows of catechol molecules (white arrows).

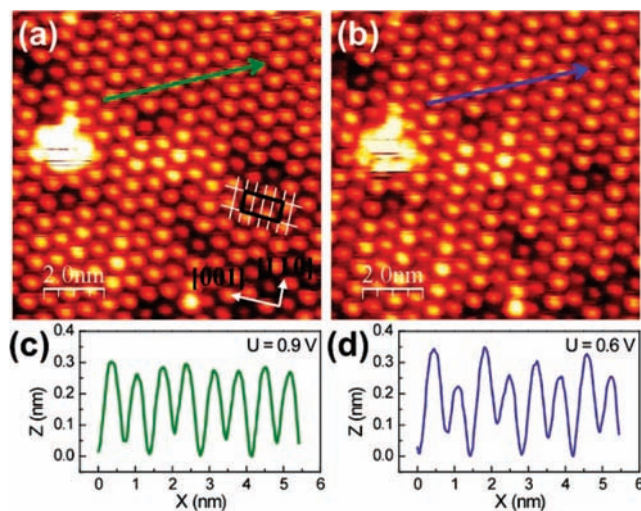


Figure 2. STM images (10×10 nm²) of a TiO₂(110) surface covered with a 4×1 overlayer of catechol, recorded on the same area with sample bias voltages of (a) +0.9 V and (b) +0.6 V and a tunneling current of ~ 0.03 nA. The green and blue arrows mark the position of the line profiles displayed in (c) and (d), respectively. The substrate and overlayer unit cells are sketched in (a).

The 4×1 superstructure constitutes a catechol coverage of half a monolayer (i.e., one catechol molecule per two TiO₂(110) unit cells), as confirmed with XPS. Interestingly, the appearance of the 4×1 superstructure depends on the tunneling conditions in STM. In part a of Figure 2, each molecule has the same apparent height, whereas every other $[1\bar{1}0]$ -oriented row appears slightly different in part b of Figure 2 using a different tunneling

(11) Perdew, J. P.; K.; Burke, *Phys. Rev. Lett.* **1996**, *77*, 3865–3868.

(12) Baroni, S.; Giannozzi, P.; De Gironcoli, S.; Dal Corso, A. *Quantum ESPRESSO*, <http://www.democritos.it>.

(13) Vanderbilt, D. *Phys. Rev. B* **1990**, *41* (11), 7892–7895.

(14) Tersoff, J.; Hamann, D. R. *Phys. Rev. B* **1985**, *31* (2), 805–813.

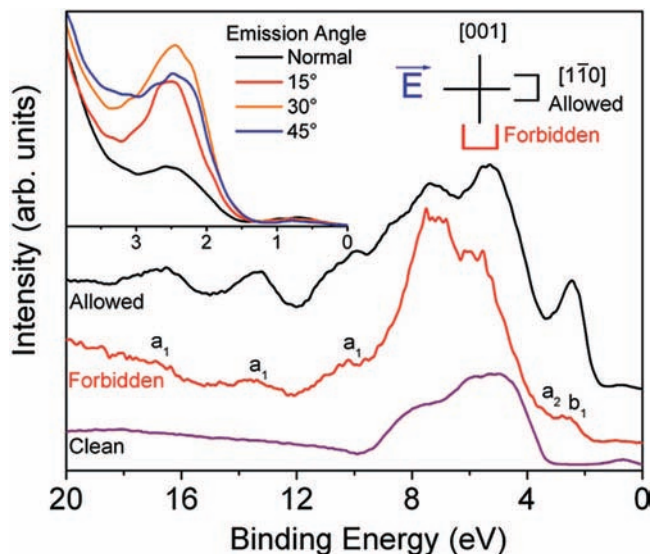


Figure 3. UV photoemission in mirror plane configuration from a clean $\text{TiO}_2(110)$ surface and after exposure to a saturation coverage of catechol at room temperature. UV light ($h\nu = 40$ eV) was incident along the sample's $[1\bar{1}0]$ direction; schematics for allowed and forbidden detector geometries are shown in the upper right-hand corner. The catechol HOMO is located at a binding energy of 2.4 eV, above the edge of the clean TiO_2 valence band. Orbital symmetries for spectral features are indicated. The inset on the top left shows the intensity variation of the HOMO states with the analyzer takeoff angle, indicating a molecular tilt ($15\text{--}30^\circ$).

voltage. As we will argue below, the difference in STM contrast is attributed to different bonding configuration of the catechol molecules.

To test the electronic structure of adsorbed catechol, we performed angle-resolved UV photoemission spectroscopy (ARUPS) using linearly polarized synchrotron radiation, as seen in Figure 3. Spectra from the clean $\text{TiO}_2(110)$ surface show a small, characteristic gap state around 0.8 eV binding energy. This state is indicative of (hydroxylated) oxygen vacancies or, possibly, titanium interstitials.¹⁵ Upon adsorption of a saturation coverage of catechol at room temperature, additional states are introduced; in particular, a peak around 2.4 eV binding energy appears in the band gap. The symmetry of this and higher binding-energy states is assigned using different sample/analyzer geometries and applying selection rules,¹⁶ as seen in Figure 3. For these mirror plane emission measurements, the sample was mounted with its $[001]$ axis in horizontal/vertical direction, that is, parallel/perpendicular to the polarization direction of the incoming synchrotron light. Spectra were taken with the electric vector, \mathbf{E} , of the incident light parallel to one major surface mirror plane, i.e. either $[001]$ or $[1\bar{1}0]$. The detector was moved parallel and perpendicular to this mirror plane, as seen in the inset of Figure 3. Thus, the photoemission signal is modulated from allowed to forbidden based on the symmetry of the initial electron wave function.¹⁶ A strong asymmetry is observed between spectra taken in the allowed and forbidden geometry with the electric vector \mathbf{E} parallel to the $[1\bar{1}0]$ direction (spectra shown in Figure 3); in particular, note the large enhancement of the catechol HOMO in the allowed geometry. The molecular orbital symmetries deduced from these measurements and corresponding data with $\mathbf{E} \parallel [001]$ are indicated in the spectra.

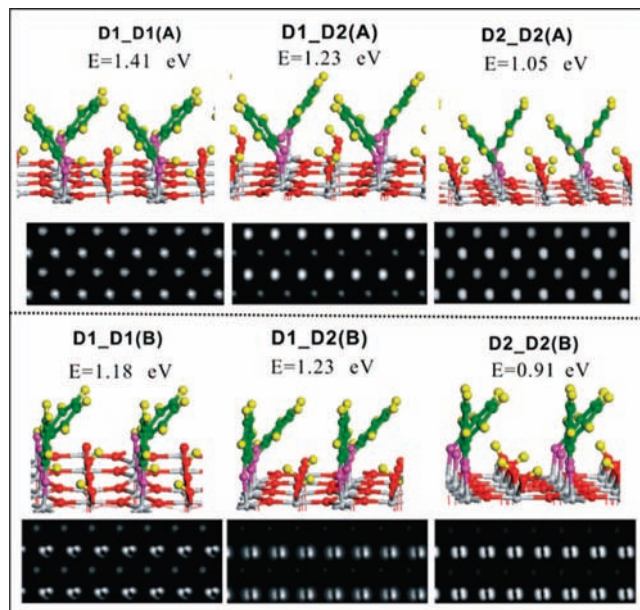


Figure 4. Calculated adsorption geometries of 0.5 monolayer of catechol on $\text{TiO}_2(110)$ with adsorption energies per molecule listed for each model. The top row shows configurations (A) where neighboring catechols are tilted in opposite directions, and in the bottom row (B) every other molecule is upright. D2 catechols are bonded in a bridging bidentate geometry, whereas molecules labeled D1 have only one dissociated hydroxyl group. Empty state simulated STM images ($V = 1.8$ eV with respect to the computed Fermi energy, see Figure 6) are shown for each structure. In these images the spots are in registry with the geometric structure shown just above, e.g. the brighter spots in the image for D1_D2(A) correspond to the D1 molecule.

From these results, we conclude that the catechol benzene ring is parallel to the $[001]$ direction of the TiO_2 surface. It also appears that the peak at 2.4 eV is composed of two states, which are assigned to the HOMO and HOMO-1 of catechol. On the basis of the emission pattern obtained from angle-resolved UPS measurements (inset Figure 3), it is concluded that the catechol molecules, which give rise to the band gap state, are tilted by $\pm 15\text{--}30^\circ$ with respect to the surface normal.

DFT calculations for low coverages ($1/4$ ML) show that the most stable structure is a completely dissociated (D2) molecule in a bidentate configuration, bridge-bonded to two Ti5c atoms of the $\text{TiO}_2(110)$ substrate. Such an isolated molecule adsorbs with an upright configuration, with the benzene ring oriented perpendicularly to the surface. With a binding energy of 1.05 eV, this configuration is more stable by 0.11 and 0.36 eV with respect to adsorbed catechol with one dissociated terminal hydroxyl (D1) and molecularly adsorbed (Mol) catechol, respectively. The densely packed phases observed experimentally were modeled with two adsorbed molecules per 4×1 unit cell, corresponding to the $1/2$ ML coverage observed experimentally. A total of nine possible adsorption geometries were examined. Structures with exclusively upright catechol molecules, as observed for isolated molecules, are not discussed here, as these configurations have a 2×1 periodicity and weak adsorption energies due to repulsive interactions between benzene rings. Figure 4 shows the optimized structures of configurations that exhibit a 4×1 periodicity; they consist of either alternating left–right tilted (upper row, A) or upright-tilted molecules (lower row, B) along the $[1\bar{1}0]$ direction (tilt angle $\sim 27^\circ$). Three dissociation combinations were considered: all catechol fully (D2_D2) or partially (D1_D1) dissociated, and a 1:1 mixture of partially and fully dissociated molecules

(15) Wendt, S.; Sprunger, P. T.; Lira, E.; Madsen, G. K. H.; Li, Z.; Hansen, J. Ø.; Matthiesen, J.; Blekinge-Rasmussen, A.; Lægsgaard, E.; Hammer, B.; Besenbacher, F. *Science* **2008**, *320*, 1755–1759.

(16) Steinruck, H.-P. *J. Phys.: Condens. Matter* **1996**, *8*, 6465–6509.

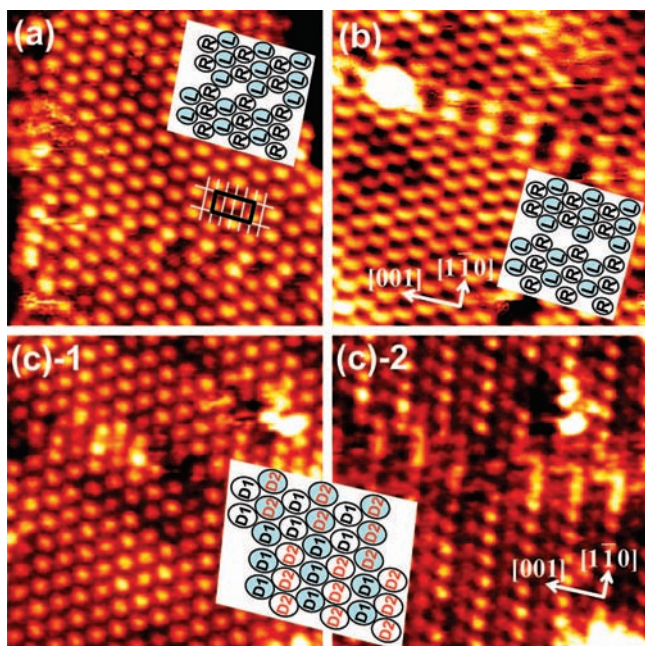


Figure 5. STM images ($10 \times 10 \text{ nm}^2$) of a $\text{TiO}_2(110)$ surface covered with a full monolayer of catechol, dosed and imaged at room temperature. The (4×1) overlayer exhibits different types of domain boundaries as sketched in the schematics. For structural domain boundaries (a, b), labels in the schematics refer to catechol as left (L) and right (R) tilted. In (a), two neighboring domains are shifted by one (substrate) unit cell along $[001]$, and the image in (b) contains a domain boundary where neighboring molecules switch from a left-tilt configuration to a right-tilt configuration when going along one $[1\bar{1}0]$ -oriented row. In (c-1), no domain boundary is visible under symmetric tunneling conditions. The same area, imaged with slightly different tunneling conditions (c-2) gives rise to a domain boundary of molecules having different (apparent) heights. Observing a domain boundary is unequivocal evidence that the height difference is due to the sample and not the STM tip.

(D1_D2). In both D1_D1 and D1_D2, H-bonding between the hydroxyl on a D1 catechol and the oxygen of the neighboring D1 or D2 molecule makes these configurations more stable than any low coverage or the D2_D2 structure. Fully molecular configurations lead to low binding energies and are not considered further.

From Figure 4, it appears that the D1_D1(A) structure with left/right tilted, monodentate catechol molecules exhibits the largest binding energy and would thus be predicted to be the most stable geometry. However, the mixed D1_D2 configurations as well as the D1_D1(B) structure are not much higher in energy, 0.18 and 0.23 eV, respectively.

To make a closer connection between theory and experiment, (empty states) STM images have been calculated; these are also reported in Figure 4. According to the simulated images, B configurations exhibit a clear difference between tilted and upright molecules, as the latter give rise to two-lobe spots reflecting the π character of the molecular states. These differences are more substantial than the subtle differences observed in the experimental images of Figure 2, suggesting that B configurations should not be present in the experiment. Images consistent with the experimental ones are instead computed for all type A configurations. In the simulated images, there are subtle differences between right- and left-tilted molecules, which depend on the voltage. However, these differences are generally small for D1_D1(A) and D2_D2(A), whereas they are quite significant for D1_D2(A). In the latter

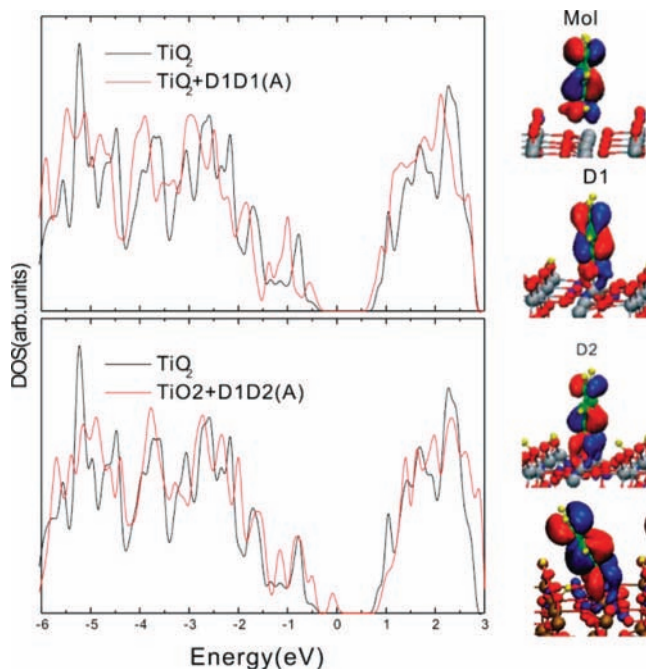


Figure 6. Total DOS of a 4×1 overlayer of catechol/ $\text{TiO}_2(110)$ in D1_D1(A) and D1_D2(A) configuration. The DOS for the clean surface (back curve) is also shown. The energy zero is the computed Fermi energy. Right panel: HOMO of catechol in different adsorption configurations at 0.25 ML coverage. From the top to the bottom: Molecular, partially dissociated monodentate D1, and fully dissociated bidentate D2, in upright configuration; bottom, bidentate tilted configuration. O atoms are red, Ti gray, C green, and H yellow.

case, the partially dissociated D1 molecule appears brighter over a wide range of voltages (Figure S1 in the Supporting Information).

We considered whether the calculated left/right tilt of the molecules could give rise to experimental artifacts resulting in STM apparent height differences; if the STM tip were asymmetric, the tunneling probability could vary for left- and right-tilted molecules, resulting in different molecules with different brightnesses in the constant-current mode employed; such an asymmetry in tunneling probability might be more pronounced for certain bias voltages. Inspection of domain boundaries (Figure 5) convinces us, however, that this is not the case and that the observed height differences must be due to *different molecular geometries* in the overlayer rather than a tip asymmetry. The experimentally observed antiphase domain boundaries shown in parts a and b of Figure 5 correspond to a shift of one and two unit cells between adjacent domains, respectively. In part c-1 of Figure 5 no domain boundary is visible under the symmetric tunneling condition. The same area, imaged with slightly different tunneling conditions, part c-2 of Figure 5, gives rise to a domain boundary of molecules having different (apparent) heights. The observation of apparent height changes across domain boundaries is unequivocal evidence that the height difference is due to the sample and not the STM tip.

It is instructive to compare the (computed) electronic structures of the two most stable configurations with tilted molecules, D1_D1(A) and D1_D2(A), as seen in Figure 6. It appears that gap states occur for the D1_D2(A) structure but not for the D1_D1(A) one. In fact, our DFT calculations predict that only *bidentate* bonded (D2) catechol gives rise to gap states; the monodentate (D1) species, whether in D1_D1 or D1_D2 conformations, does *not* introduce states into the band gap. By

combining this with the STM and UPS findings, we conclude that both D1_D1(A) and D1_D2(A) structures should be present in the experiment. On the basis of constrained minimization calculations, the barrier for transition from D1_D2(A) to the most stable D1_D1(A) structure is estimated as ~ 0.21 eV. Thus, these two structures can easily convert from one into the other via proton exchange between the surface and the adsorbed catechol. We also note that, although energetically less stable, D1_D2(A) should be entropically more favorable than D1_D1(A).

To understand the origin of the gap states for bidentate catechol, we carried out a detailed analysis of the geometric structures, projected densities of states, and molecular orbital charge densities for the adsorbed catechol–TiO₂ system at both 0.25 and 0.5 ML coverages. For molecularly adsorbed catechol (Mol), we find that the HOMO is a π state that lies about 0.4 eV below the top of the TiO₂ valence band (E_v). This is consistent with the fact that the measured ionization energy, 8.17–8.56 eV, of gas phase catechol¹² is larger than that of an electron at the top of the TiO₂ valence band, which is in the range 7.5–8 eV.³ In the D1 and D2 configurations, with one and two dissociated hydroxyl groups, respectively, the catechol HOMO couples to 3d states on the Ti atoms to which the molecule is bonded (see the isosurface plots on the right of Figure 6). As a result, the HOMO moves up in energy; it is ~ 0.1 eV below E_v in the D1 configuration but moves further up and lies above E_v in the D2 configuration. This destabilization of the catechol HOMO is a feature that has been found in theoretical studies using different electronic structure approaches, and is largely independent of the choice of the DFT functional.^{8,17}

The same mechanism of gap-state formation that we have outlined above for catechol applies to other molecules, for example alizarin¹⁷ and glucose,¹⁸ for which binding to the surface occurs via two Ti–O bonds formed upon dissociation

of two molecular hydroxyls. By contrast, no gap state is present for molecules like phenol and benzoic acid,^{4,8} for which adsorption requires dissociation of a single molecular OH group. The adsorbate-induced occupied states in the TiO₂ band gap are important in photocatalysis because they are efficient traps for photogenerated holes. This suggests that catechol adsorbed in bidentate form is more easily photo-oxidized than catechol adsorbed in molecular or monodentate form. The catechol-induced gap states are also relevant for charge transfer in DSSCs. Photoexcitation from these occupied states can lead to efficient direct charge injection into TiO₂ at sub-bandgap energies.⁸ However, the coupling of these states to the TiO₂ semiconductor may also favor the back transfer of the photoexcited carrier to the dye, a detrimental effect for the performance of DSSCs.

5. Summary

In summary, combining DFT calculations with UPS and STM measurements, we have found that catechol adsorbed on TiO₂(110) can form two different full-coverage H-bonded structures, comprising either monodentate only or mixed monodentate–bidentate molecules. These two structures can easily convert from one into the other via proton exchange between the surface and the adsorbed catechol. There is an important correlation between the electronic structure, the adsorption geometry, and the degree of dissociation of the molecules. This correlation can play a significant role in photocatalysis and DSSCs.

Acknowledgment. This work was supported by the Department of Energy (DE-FG02-05ER15702).

Supporting Information Available: Additional STM calculations and DOS calculations over a wider energy range. This material is available free of charge via the Internet at <http://pubs.acs.org>.

JA803595U

(17) Duncan, W. R.; Prezhdo, O. V. *J. Phys. Chem. B* **2005**, *109*, 365–373.

(18) Du, M.-H.; Feng, J.; Zhang, S. B. *Phys. Rev. Lett.* **2007**, *98*, 066102.